Modeling the Active Sites in Metalloenzymes. 3. Density Functional Calculations on Models for [Fe]-Hydrogenase: Structures and Vibrational Frequencies of the Observed Redox Forms and the Reaction Mechanism at the Diiron Active Center

Zexing Cao[†] and Michael B. Hall*

Contribution from the Department of Chemistry, Texas A&M University, College Station, Texas 77843

Received January 10, 2000. Revised Manuscript Received June 29, 2000

Abstract: Optimized structures for the redox species of the diiron active site in [Fe]-hydrogenase as observed by FTIR and for species in the catalytic cycle for the reversible H_2 oxidation have been determined by density-functional calculations on the active site model, $[(L)(CO)(CN)Fe(\mu\text{-PDT})(\mu\text{-CO})Fe(CO)(CN)(L')]^q$ ($L = H_2O$, CO, H_2, H^-; PDT = $SCH_2CH_2CH_2S$, $L' = CH_3S^-$, CH_3SH; $q = 0, 1-, 2-, 3-$). Analytical DFT frequencies on model complexes $(\mu\text{-PDT})Fe_2(CO)_6$ and $[(\mu\text{-PDT})Fe_2(CO)_4(CN)_2]^{2-}$ are used to calibrate the calculated CN^- and CO frequencies against the measured FTIR bands in these model compounds. By comparing the predicted CN^- and CO frequencies from DFT frequency calculations on the active site model with the observed bands of *D. vulgaris* [Fe]-hydrogenase under various conditions, the oxidation states and structures for the diiron active site are proposed. The fully oxidized, EPR-silent form is an Fe(II)-Fe(II) species. Coordination of H_2O to the empty site in the enzyme's diiron active center results in an oxidized inactive form (H_2O)Fe-(II)-Fe(II). The calculations show that reduction of this inactive form releases the H_2O to provide an open coordination site for H_2. The partially oxidized active state, which has an $S = {}^1/_2$ EPR signal, is an Fe(I)-Fe(II) species. Fe(I)-Fe(I) species with and without bridging CO account for the fully reduced, EPR-silent state. For this fully reduced state, the species without the bridging CO is slightly more stable than the structure with the bridging CO. The correlation coefficient between the predicted CN^- and CO frequencies for the proposed model species and the measured CN^- and CO frequencies in the enzyme is 0.964. The proposed species are also consistent with the EPR, ENDOR, and Mössbauer spectroscopies for the enzyme states. Our results preclude the presence of Fe(III)-Fe(II) or Fe(III)-Fe(III) states among those observed by FTIR. A proposed reaction mechanism (catalytic cycle) based on the DFT calculations shows that heterolytic cleavage of H_2 can occur from $(\eta^2\text{-}H_2)$Fe(II)-Fe(II) via a proton transfer to "spectator" ligands. Proton transfer to a CN^- ligand is thermodynamically favored but kinetically unfavorable over proton transfer to the bridging S of the PDT. Proton migration from a metal hydride to a base (S, CN, or basic protein site) results in a two-electron reduction at the metals and explains in part the active site's dimetal requirement and ligand framework which supports low-oxidation-state metals. The calculations also suggest that species with a protonated Fe−Fe bond could be involved if the protein could accommodate such species.

Introduction

[Ni-Fe] hydrogenases and [Fe]-hydrogenases are two major classes of metalloproteins which catalyze the reversible activation of molecular hydrogen according to the reaction $H_2 \leftrightarrow 2H^+ + 2e^-$. In living systems, the [Ni−Fe] enzymes are mainly used to oxidize H_2, while the Fe-only enzymes are mainly used to reduce H^+.[1−4] Among these two classes of hydrogenases, the [Ni-Fe] enzymes have received more attention both experimentally and theoretically.[3,5−9] Different redox states in the catalytic cycle of the [Ni-Fe]-hydrogenase enzymes have been experimentally characterized and structural models have been proposed for each of the observed intermediates.[6] The less well studied Fe-only enzymes are now known to contain at least two [4Fe-4S] clusters and an unusual iron−sulfur cluster, the so-called H cluster, at the active site.

[†] Permanent address: Department of Chemistry, State Key Laboratory for Physical Chemistry of the Solid Surface, Xiamen University, Xiamen 361005, China.

(1) (a) Adams, M. W. W. *Biochim. Biophys. Acta* **1990**, *1020*, 115. (b) Adams, M. W. W.; Stiefel, E. I. *Science* **1998**, *282*, 1842.

(2) Albracht, S. P. J. *Biochim. Biophys. Acta* **1994**, *1118*, 167.

(3) Frey, M. *Structure and Bonding*; Springer-Verlag: Berlin, Heidelberg, 1998; Vol. 90, p 97.

(4) Cammack, R. *Nature* **1999**, *397*, 214.

(5) (a) De Lacey, A. L.; Hatchikian, E. C.; Volbeda, A.; Frey, M.; Fontecilla-Camps, J. C.; Fernandez, V. M. *J. Am. Chem. Soc.* **1997**, *119*, 7181. (b) Volbeda, A.; Charon, M. H.; Pieras, C.; Hatchikian, E. C.; Frey, M.; Fontecilla-Camps, J. C. *Nature* **1995**, *373*, 580. (c) Volbeda, A.; Garcin, E.; Piras, C.; De Lacey, A. I.; Fernandez, V. M.; Hatchikian, E. C.; Frey, M.; Fontecilla-Camps, J. C. *J. Am. Chem. Soc.* **1996**, *118*, 12989. (d) Happe, R. P.; Roseboom, W.; Pierik, A. J.; Albracht, S. P. J. *Nature* **1997**, *385*, 126. (e) Bagley, K. A.; Van Garderen, C. J.; Chen, M.; Duin, E. C.; Albracht, S. P. J.; Woodruff, W. H. *Biochemistry* **1994**, *33*, 9229. (f) Bagley, K. A.; Duin, E. C.; Roseboom, W.; Albracht, S. P. J.; Woodruff, W. H. *Biochemistry* **1995**, *34*, 5527.

(6) (a) Niu, S.; Thomson, L. M.; Hall, M. B. *J. Am. Chem. Soc.* **1999**, *121*, 4000. (b) Li, S.; Hall, M. B. *Inorg. Chem.* **2001**, *40*, 18. (c) Fan, J.; Hall, M. B. *J. Bio. Inorg. Chem.*, in press.

(7) (a) Pavlov, M.; Siegbahn, P. E. M.; Blomberg, M. R. A.; Crabtree, R. H. *J. Am. Chem. Soc.* **1998**, *120*, 548. (b) Pavlov, M.; Blomberg, M. R. A.; Siegbahn, P. E. M. *Int. J. Quantum Chem.* **1999**, *73*, 197.

(8) De Gioia, L.; Fantucci, P.; Guigliarelli, B.; Bertrand, P. *Inorg. Chem.* **1999**, *38*, 2658.

(9) Amara, P.; Volbeda, A.; Fontecilla-Camps, J. C.; Field, M. J. *J. Am. Chem. Soc.* **1999**, *121*, 4468.

10.1021/ja000116v CCC: $20.00
Published on Web 04/18/2001

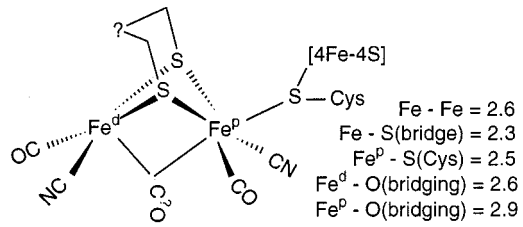

Figure 1. A composite structure for the active site based on the crystal structures of [Fe]-hydrogenase.

Table 1. Observed FTIR Bands of *D. vulgaris* [Fe]-Hydrogenase[a]

CN^-	CO	condition[b]
2106(s)[c]	2008(s)	air
2087(s)	1983(s)	
	1848(s)	
2095(w)	2016(w)	H_2/Ar
2079(w)	1972(w)	
	1965(s)	
	1940(s)	
2096(s)	2016(s)	H_2/CO
2088(s)	1971(s)	
	1964(s)	
	1811(s)	
2079(w)	1965(w)	H_2
2041(w)	1941(w)	
	1916(w)	
	1894(s)	

[a] From ref 10. [b] Air: In air without additional treatment. H_2/Ar: After complete replacement of H_2 by Ar. H_2/CO: After complete replacement of H_2 by CO. H_2: After reduction with H_2 for 3 h at room temperature. [c] Relative intensities (s, strong; w, weak).

A variety of experimental techniques have been applied to the H cluster.[1] These studies indicate that the H-cluster proteins from different organisms are essentially the same. Infrared spectroscopic studies on the [Fe] hydrogenases from *Desulfovibrio vulgaris* (DvHase),[10] as well as X-ray crystal structures of Fe-only hydrogenases isolated from *Clostridium pasteurianum* (CpHase)[11] and *Desulfovibrio desulfuricans* (DdHase),[12] suggest that the active site of Fe-only hydrogenases contains diatomic ligands, CN^- and CO. Figure 1 embodies features of the distal−proximal diiron site (Fe^d-Fe^p) from both CpHase and DdHase structures. IR bands of the active site from DvHase under various conditions are listed in Table 1. Similarities in the infrared spectroscopy, the peptide sequence, and the X-ray structures at the H cluster support the generalized structure shown in Figure 1,[12] even though assignment of the bridging groups remains somewhat ambiguous in both of the X-ray studies.[11,12]

It is known that the fully oxidized inactive H cluster and the completely reduced (by H_2) H cluster are EPR silent, while the partially oxidized active H cluster is paramagnetic.[10c] The spin and oxidation states of the diiron cluster and the proximal [4Fe-4S] cluster in different redox forms of [Fe]-hydrogenase are still controversial. On the basis of Mössbauer,[13a−b] EPR,[13c−e] and ENDOR[13f−h] spectroscopic studies of the H cluster in [Fe]-hydrogenases, Popescu and Münck argue that the [4Fe-4S] subcluster of the [2Fe-2S]−[4Fe-4S] assembly carries a 2+ charge in both oxidized and reduced forms of the H cluster.[13a] They suggest that the diamagnetic, fully reduced state of the diiron site is a low-spin Fe(II)-Fe(II) pair, while the partially oxidized, active diiron cluster is most likely in the mixed-valence Fe(III)-Fe(II) state. In this oxidized state, the H cluster exhibits an $S = {}^1/_2$ EPR signal, where the $S = {}^1/_2$ spin is centered at the Fe(III) site distal to the [4Fe-4S] cluster. However, they offer the possibility that "an Fe^IFe^I/Fe^IFe^{II} redox couple" could accommodate their results.[13] In contrast, Nicolet et al.[12] argued that the [4Fe-4S] cluster in the oxidized and reduced enzyme carries a 1+ charge. They further argue that in the oxidized active state of the H cluster the Fe ions of the binuclear center could be "either ferrous intermediate spin ($S = 1$) or, more likely, ferric low spin ($S = {}^1/_2$)."[12]

Recent studies by Darensbourg and co-workers,[14] by Rauchfuss and co-workers,[15a] and by Pickett and co-workers[15b] show that Fe(I)-Fe(I) model complexes such as $[(\mu\text{-PDT})Fe_2(CO)_6]$ and $[(\mu\text{-PDT})Fe_2(CO)_4(CN)_2]^{2-}$ are stable and structurally similar to the iron dimer of the H cluster. Moreover, inspection of the FTIR spectra of the oxidized inactive *D. vulgaris* [Fe]-hydrogenase[10] isolated in air reveals that these bands are comparable with the FTIR spectra of Fe(II) organometallic complexes which are excellent analogues to the Fe(II) center of [NiFe]-hydrogenases.[16]

The enzymatic cleavage of H_2 at the active site has been presumed to be heterolytic and assisted by a base.[17,18a,b] Because the only close base, Lys237 at 4.4 Å, is far from Fe^d (distal), Nicolet and co-workers suggested that the putative CN^- ligand could bind a proton first, subsequently transferring it to other residues.[12] Kubas and co-workers[18b] reported H_2 binding and cleavage on highly electrophilic organometallic complexes which contain strong π-acceptor ligands such as CO. They assumed that the heterolytic cleavage of H_2 occurs on a low-spin d^6 Fe(II) and that the proton jumps to a deprotonated cysteine(299) sulfur site located in close proximity (3 Å) to the H_2 binding site for reversible H_2 consumption/production in *C. pasteurianum*.

Previously, by combining DFT calculations on Fe(II) organometallic models with those on [Ni-Fe] active site models, we were able to determine the metal oxidation states and degree of protonation at the [Ni-Fe] enzyme's active site.[6] We showed

(10) (a) Pierik, A. J.; Hulstein, M.; Hagen, W. R.; Albracht, S. P. J. *Eur. J. Biochem*. **1998**, *258*, 572. (b) Van der Spek, T. M.; Arendsen, A. F.; Happe, R. P.; Yun, S.; Bagley, K. A.; Hagen, W. R.; Albracht, S. P. J. *Eur. J. Biochem*. **1996**, *237*, 629. (c) Pierik, A. J.; Hagen, W. R.; Redeker, J. S.; Wolbert, R. B. G.; Boersma, M.; Verhagen, M. F. J. M.; Grande, H. J.; Veeger, C.; Mutsaers, P. H. A.; Sand, R. H.; Dunham, W. R. *Eur. J. Biochem*. **1992**, *209*, 63.

(11) Peters, J. W.; Lanzilotta, W. N.; Lemon, B. J.; Seefedt, L. C. *Science* **1998**, *282*, 1853. Peters, J. W.; Lanzilotta, W. N.; Lemon, B. J.; Seefedt, L. C. *Science* **1999**, *283*, 35. Peters, J. W.; Lanzilotta, W. N.; Lemon, B. J.; Seefedt, L. C. *Science* **1999**, *283*, 2102.

(12) Nicolet, Y.; Piras, C.; Legrand, P.; Hatchikian, C. E.; Fontecilla-Camps, J. C. *Structure* **1999**, *7*, 13.

(13) (a) Popescu, C. V.; Münck, E. *J. Am. Chem. Soc*. **1999**, *121*, 7877. (b) Rusnak, F. M.; Adams, M. W. W.; Mortenson, L. E.; Münck, E. *J. Biol. Chem*. **1987**, *262*, 38. (c) Adams, M. W. W.; Mortenson, L. E. *J. Biol. Chem*. **1984**, *259*, 7045. (d) Adams, M. W. W. *J. Biol. Chem*. **1987**, *262*, 15054. (e) Zambrano, I. C.; Kowal, A. T.; Mortenson, L. E.; Adams, M. W. W.; Johnson, M. K. *J. Biol. Chem*. **1989**, *264*, 20974. (f). Telser, J.; Benecky, M. J.; Adams, M. W. W.; Mortenson, L. E.; Hoffman, B. M. *J. Biol. Chem*. **1987**, *262*, 6589. (g) Wang, G.; Benecky, M. J.; Huynh, B. H.; Cline, J. F.; Adams, M. W. W.; Mortenson, L. E.; Hoffman, B. M.; Münck, E. *J. Biol. Chem*. **1984**, *259*, 14328−14331. (h) Telser, J.; Benecky, M. J.; Adams, M. W. W.; Mortenson, L. E.; Hoffman, B. M. *J. Biol. Chem*. **1986**, *261*, 13536−13541.

(14) Lyon, E. J.; Georgakaki, I. P.; Reibenspies, J. H.; Darensbourg, M. Y. *Angew. Chem., Int. Ed*. **1999**, *38*, 3178.

(15) (a) Rauchfuss, T. B.; Contakes, S. M.; Schmidt, M. *J. Am. Chem. Soc*. **1999**, *121*, 9736. (b) Cloirec, A. L.; Best, S. P.; Borg, S.; Davies, S. C.; Evans, D. J.; Hughes, D. L.; Pickett, C. J. *Chem. Commun*. **1999**, 2285.

(16) Lai, C.-H.; Lee, W.-Z.; Miller, M. L.; Reibenspies, J. H.; Darensbourg, D. J.; Darensbourg, M. Y. *J. Am. Chem. Soc*. **1998**, *120*, 10103.

(17) Adams, M. W.; Mortenson, L. E.; Chen, L. S. *Biochim. Biophys. Acta* **1980**, *594*, 105.

(18) (a) Crabtree, R. H. *Inorg. Chem. Acta Biorg.* **1986**, *125*, L7. (b) Huhmann-Vincent, J.; Scott, B. L.; Kubas, G. J. *Inorg. Chim. Acta* **1999**, *294*, 240. (c) Fauvet, K.; Mathieu, R.; Poilblanc, R. *Inorg. Chem.* **1976**, *15*, 976. (d) Arabi, M. S.; Mathieu, R.; Poilblanc, R. *J. Organomet. Chem.* **1979**, *177*, 199.

that the low-spin Fe(II) site with π-accepting ligands was the most favorable site for H_2 capture. This study also suggested that the Ni center is oxidized to Ni(III) before heterolytic H_2 cleavage occurs leaving a hydride between the metals and a proton on a terminal S. Others have come to similar conclusions.[7,8] Very recently, Dance[19] reported density functional calculations on the diiron model $CH_3S(CO)(CN)FeS_2(\mu\text{-}CO)$-$Fe(CO)(CN)$. A relatively flat potential energy surface for geometric change at Fe, CO, S, and bound H was calculated. Because *D. desulfuricans* [Fe]-hydrogenase appears to have a dithiolate bridge $-SCH_2CH_2CH_2S-$ (PDT), use of an $(S^{2-})_2$ bridge results in a more negative charge on this diiron cluster model in comparison with the H cluster.

To rationalize the structural features of various redox states of the diiron center and the mechanism of enzymatic cleavage of H_2 at the diiron center, we carried out theoretical calculations on the diiron model $[(L)(CO)(CN)Fe(\mu\text{-PDT})(\mu\text{-CO})Fe(CO)$-$(CN)(L')]^q$ ($L = H_2O$, CO, H_2, H^-; $L' = CH_3S^-$, CH_3SH; PDT $= SCH_2CH_2CH_2S$; $q = 0, 1-, 2-, 3-$). The optimized geometries of possible redox states and the species involved in the catalytic cycle, as well as the predicted infrared spectra of relevant species, are reported. By combining the experimental data on both the model complexes and the enzyme with predictions from density functional theory (DFT), we can select candidate species for various observed redox states of the diiron cluster in [Fe]-hydrogenases. Mechanisms for cleavage of H_2 and proton-transfer paths are also proposed.

Computational Details

The geometries have been optimized by DFT, specifically with the Becke[20] three-parameter hybrid exchange functional and the Lee−Yang−Parr[21] correlation function (B3LYP). Vibrational frequency analyses were performed within an analytic formalism to predict IR bands of nonprotein ligands, CO and CN^-, in relevant redox states.

Iron is described by the Hay and Wadt basis set with effective core potentials (ECP).[22] The 4p orbital in the ECP basis set was replaced by optimized (41) split valence functions from Couty and Hall.[23] This modified ECP basis set of Fe was augmented by an f polarization function.[24] For CO and CN^- ligands, the Hay and Huzinaga D95V* basis sets were employed.[25] A standard 3-21G basis set was used to describe $CH_2CH_2CH_2$ in the μ-PDT group and CH_3 in SCH_3, as well as H_2O bound to the active site. For reactive hydrogen, the 6-311G** basis set was used. Three types of basis sets, including 6-31G, Lanl2DZ*, and 6-31G*, were considered for S. Calculations on model compounds show that the Lanl2DZ* basis set predicts nearly the same optimized geometries as an all-electron 6-31G* basis set. Thus, the Lanl2DZ* for S was used in all calculations.

To simulate the possibility that the proximal [4Fe-4S] cube serves as an oxidation-level buffer, CH_3S^- and CH_3SH groups are employed to model Cys-S-[4Fe-4S] in Figure 1. The use of these alternative ligands also simulates other changes in the active site environment, such as H-bonding and solvation effects. Furthermore, although our model uses PDT as the dithiolate bridge, this ligand has not been unambiguously confirmed by experimental studies. All DFT calculations were performed with GAUSSIAN 98 programs,[26] at the Supercomputer Facility of Texas A&M University.

Results and Discussion

Calibration of the Calculated CO and CN^- Frequencies. To set up a relationship between the calculated and measured CO and CN^- frequencies in systems with Fe−CO and Fe−CN bonds similar to those in Fe-only hydrogenases, we optimized the structures of two model complexes $[Fe_2(CO)_6(\mu\text{-PDT})]$ (**A**) and $[Fe_2(CO)_4(CN)_2(\mu\text{-PDT})]^{2-}$ (**B**), which were synthesized and studied by Darensbourg, Rauchfuss, Pickett, and their coworkers.[14,15] Although these model systems do not provide a bridging CO similar to that proposed for the active site in the H cluster, they are the best available analogues with Fe-bound CO, CN^-, and S ligands similar to those found in the active site. DFT calculations show an excellent agreement between the optimized geometries and the crystal structure and an excellent correlation between the calculated frequencies and the observed bands (Figure 2). For models **A** and **B**, Table 2 shows a comparison of the calculated and predicted frequencies with the observed bands, the calculated and observed intensities, and the assignments for these vibrational modes. Small splittings

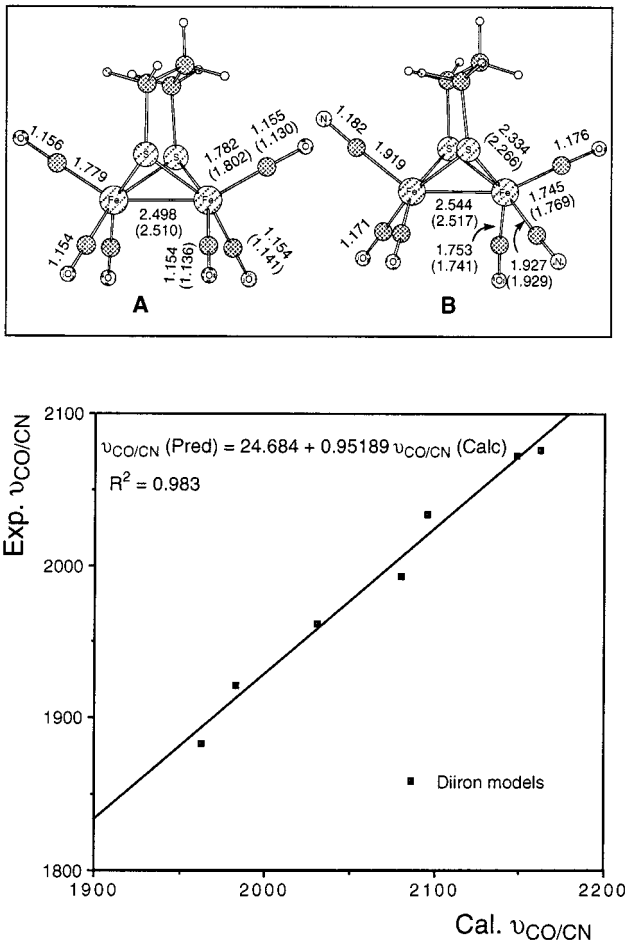

Figure 2. Experimental and DFT optimized geometries (Å, experimental values in parentheses) of the model compounds $[Fe_2(CO)_6(\mu\text{-PDT})]$ and $[Fe_2(CO)_4(CN)_2(\mu\text{-PDT})]^{2-}$ are shown at the top. Correlation of the calculated and observed CN^- and CO frequencies (cm^{-1}) of the model compounds are shown at the bottom.

(19) Dance, I. *Chem. Commun.* **1999**, 1655.
(20) Becke, A. D. *J. Chem. Phys.* **1993**, *98*, 5648.
(21) Lee, C.; Yang, W.; Parr, R. G. *Phys. Rev.* **1988**, *B37*, 785.
(22) Hay, P. J.; Wadt, W. R. *J. Chem. Phys.* **1985**, *82*, 299.
(23) Couty, M.; Hall, M. B. *J. Comput. Chem.* **1996**, *17*, 1359.
(24) Höllwarth, A.; Böhme, M.; Dapprich, S.; Ehlers, A. W.; Gobbi, A.; Jonas, V.; Köhler, K. F.; Stegmann, R.; Veldkamp, A.; Frenking, G. *Chem. Phys. Lett.* **1993**, *208*, 111.
(25) Dunning, T. H., Jr.; Hay, P. J. In *Modern Theoretical Chemistry*; Schaefer, F. F., III, Ed.; Plenum: New York, 1976; Vol. 3, p 1.
(26) Frisch, M. J.; Trucks, G. W.; Schlegel, H. B.; Scuseria, G. E.; Robb, M. A.; Cheeseman, J. R.; Zakrzewski, V. G.; Montgomery, J. A., Jr.; Stratmann, R. E.; Burant, J. C.; Dapprich, S.; Millam, J. M.; Daniels, A. D.; Kudin, K. N.; Strain, M. C.; Farkas, O.; Tomasi, J.; Barone, V.; Cossi, M.; Cammi, R.; Mennucci, B.; Pomelli, C.; Adamo, C.; Clifford, S.; Ochterski, J.; Petersson, G. A.; Ayala, P. Y.; Cui, Q.; Morokuma, K.; Malick, D. K.; Rabuck, A. D.; Raghavachari, K.; Foresman, J. B.; Cioslowski, J.; Ortiz, J. V.; Stefanov, B. B.; Liu, G.; Liashenko, A.; Piskorz, P.; Komaromi, I.; Gomperts, R.; Martin, R. L.; Fox, D. J.; Keith, T.; Al-Laham, M. A.; Peng, C. Y.; Nanayakkara, A.; Gonzalez, C.; Challacombe, M.; Gill, P. M. W.; Johnson, B. G.; Chen, W.; Wong, M. W.; Andres, J. L.; Gonzalez, C.; Head-Gordon, M.; Replogle, E. S.; Pople, J. A. Gaussian, Inc.: Pittsburgh, PA, 1998.

Table 2. Calculated, Predicted, and Observed CN^- and CO Frequencies (cm^{-1}, Intensities in km/mol) for the Diiron Models [(μ-PDT)$Fe_2(CO)_6$] (**A**) and [(μ-PDT)$Fe_2(CO)_4(CN)_2]^{2-}$ (**B**)

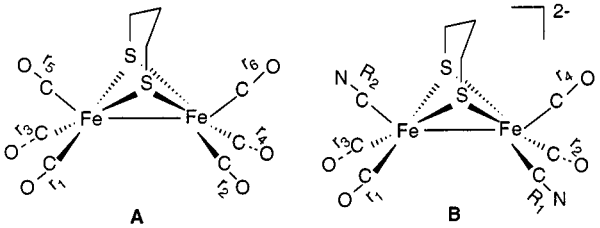

	calcd (intensity)		predicted[a]		experiment[b]		
model	CN^-	CO	CN^-	CO	CN^-	CO	assignment[c]
A		2148 (586)		2069		2072	$r_1 + r_2 + r_3 + r_4 + r_5 + r_6$
		2099 (2038)		2020		2033	$r_2 + r_4 + r_6 - (r_1 + r_3 + r_5)$
		2093 (1218)		2017		2033	$r_1 + r_2 - (r_3 + r_4)$
		2080 (866)		2005		1993	$r_5 + r_6 - (r_1 + r_2 + r_3 + r_4)$
		2076 (0.0)		2000			$r_1 + r_4 - (r_2 + r_3)$
		2070 (55)		1995			$r_2 + r_4 + r_5 - (r_1 + r_3 + r_6)$
B	2167 (122)	2031 (1044)	2087	1958	2076	1962	R_1; $r_1 + r_2 + r_3 + r_4$
	2157 (156)	1983 (1532)	2078	1912	2076	1921	R_2; $r_1 - (r_2 + r_3 + r_4)$
		1963 (1628)		1893		1883	$r_2 + r_4 - (r_1 + r_3)$
		1944 (406)		1875			$r_3 + r_4 - r_2$

[a] $\nu_{CO/CN}$ (predicted) = 24.684 + 0.95189 $\nu_{CO/CN}$(calcd). [b] References 14 and 15. [c] r_i (i = 1,6) and R_i (i = 1,2) indicate the CO and CN bonds, respectively.

of a pair of CO bands in complex **A** and the CN^- bands in complex **B** are not observed in the experiment. By combining the experimental spectra on the H cluster with CO and CN^- bands predicted by applying this correlation to active site DFT calculations, we may sort out plausible redox states. Previous work comparing CO bands from DFT calculations on model compounds with those of the [Ni-Fe] enzyme suggests that the difference in the environment between enzyme and model system causes systematic shifts of CO (and CN^-) frequencies to lower frequency than those predicted by the calculations on the model compounds.[6] A similar shift to lower frequencies has also been observed when in protein and in vacuum active-site clusters are compared.[9]

Possible Forms of Redox States. The optimized structures for various redox states of the active-site model (L)(CO)(CN)-Fe(μ-PDT)(μ-CO)Fe(CO)(CN)(L′) are shown in Figure 3. Generally, the Fe−Fe distance in these species varies from 2.5 to 3.2 Å. Table 3 lists the predicted frequencies for most of the species in Figure 3. In assigning oxidation states, we viewed all CO ligands as neutral, even the bridging CO which has significant acyl character in some species.

Oxidized EPR Silent State. The DvHase enzyme when isolated in air is inactive, but it can be activated by reduction.[27] It is known that the fully oxidized inactive enzyme and completely reduced enzyme (by H_2) are EPR silent at the active site.[10c,13,28] Since Fe-only hydrogenases are found in anaerobic organisms and are usually sensitive to dioxygen, the DvHase enzyme as isolated in air is likely the fully oxidized inactive enzyme. Table 1 presents the FTIR bands of DvHase [Fe]-hydrogenase under different conditions.[10a] Five fairly strong bands for the DvHase enzyme isolated in air were observed. The two weaker bands at 2106 and 2087 cm^{-1} are assigned to terminal CN^- groups. The two stronger bands around 2000 cm^{-1} were assigned to terminal COs, while the lower frequency band at 1848 cm^{-1} was assigned to a bridging CO; bridging COs typically have lower frequencies than terminal COs.[29,30] These Fe-bound CN^- and CO bands are comparable to the IR bands of Fe(II) organometallic compexes.[16]

Among the higher oxidized state species shown in Figure 3, species **3**, an Fe(II)-Fe(II) species, would be EPR silent and has two predicted CN^- bands at 2126 and 2105 cm^{-1}, two terminal CO bands at 2030 and 2019 cm^{-1}, and a bridging CO band at 1912 cm^{-1}. These predicted bands may be correlated with observed CN^- bands of 2106 and 2087 cm^{-1} and CO bands at 2008, 1983, and 1848 cm^{-1} in the oxidized inactive DvHase enzyme as isolated in air. As mentioned above, we expect the frequencies in the enzyme to be 20 cm^{-1} (or more) lower in frequency than predictions based on the model complexes. Thus, the Fe(II)-Fe(II) species **3** is a possible candidate for the diiron center of the oxidized inactive DvHase enzyme. The corresponding CN^- and CO bands for the Fe(III)-Fe(II) species **1** and Fe(II)-Fe(II)′ species **2** (Table 3) are too high in frequency when compared with observed bands of the oxidized enzyme in air (Fe′ refers to protonation of the L′ = CH_3S^- group, so that L′ = CH_3SH, a procedure that we use to mimic changes in the oxidation state of the Fe_4S_4 cluster attached to this S in the enzyme or other environmental changes near the active site). Moreover, FTIR spectra support the existence of a bridging CO, which is not present in either **1** or **2**, for the oxidized inactive form of DvHase in air. Although **1** would be EPR active (in contrast to the observed behavior of the oxidized form), an EPR inactive Fe(III)-Fe(III) species would have even higher CN^- and CO frequencies, totally incompatible with the experimental frequencies. Attempts to calculate the structure of an Fe(III)-Fe(III) species similar to **1**−**3** resulted in the formation of a disulfide bond, i.e., the sulfurs reduced the irons back to Fe(II)-Fe(II). Thus, the EPR-silent, oxidized form of the H cluster must be an Fe(II)-Fe(II) species such as **3**.

Coordination of H_2O to the empty site of the Fe(II)-Fe(II) species **3** forms the complex (H_2O)Fe(II)-Fe(II), **4**, with an exothermicity of −23 kcal/mol. In this stable complex **4**, H_2O

(27) Van der Westen, H. M.; Mayhew, S. G.; Veeger, C. *FEBS Lett*. **1978**, *86*, 122.
(28) Patil, D. S.; Moura, J. J. G.; He, S. H.; Teixeira, M.; Prickril, B. C.; DerVartanian, D. V.; Peck, H. D., Jr.; LeGall, J.; Huynh, B. H. *J. Biol. Chem*. **1988**, *263*, 18732.
(29) Cotton, F. A.; Wilkinson, G. *Advanced Inorganic Chemistry*; Wiley: New York, 1988.
(30) Nakamoto, K.; *Infrared and Raman Spectra of Inorganic and Coordination Compounds*; Wiley: New York, 1997.

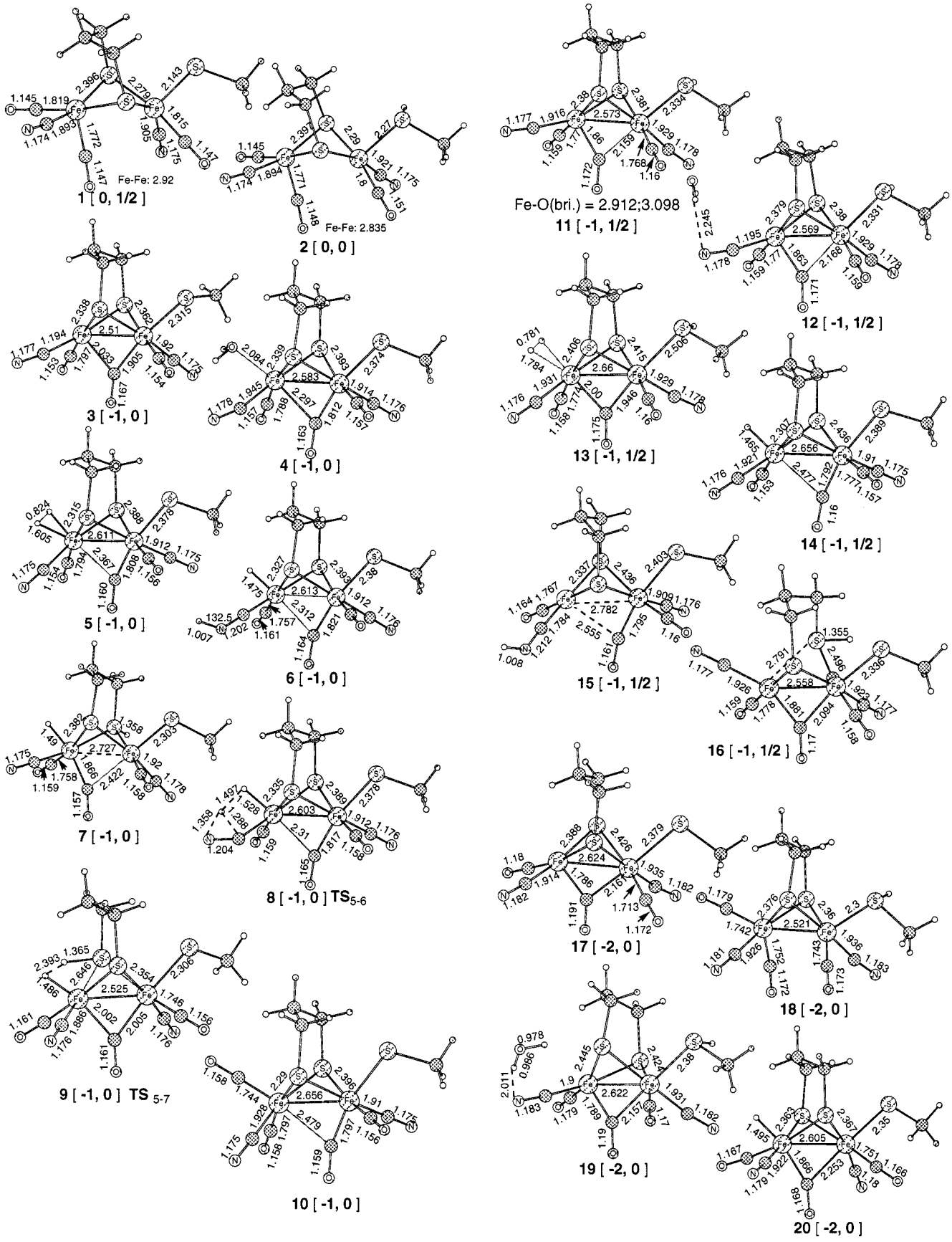

occupies the empty coordination site of the diiron center, the site that is presumed to be responsible for binding and activation of H_2. The presence of H_2O strongly bound to the active site in **4** blocks binding of H_2 and results in an inactive oxidized enzyme. The Fe(II)-Fe(II) species **3** can bind a molecular H_2 or CO to form stable complexes (η^2-H_2)Fe(II)-Fe(II), **5**, or (CO)-Fe(II)-Fe(II), **10**, with exothermicities of −16.4 and −45.4 kcal/mol, respectively. The (η^2-H_2)Fe(II)-Fe(II) species **5** may be a

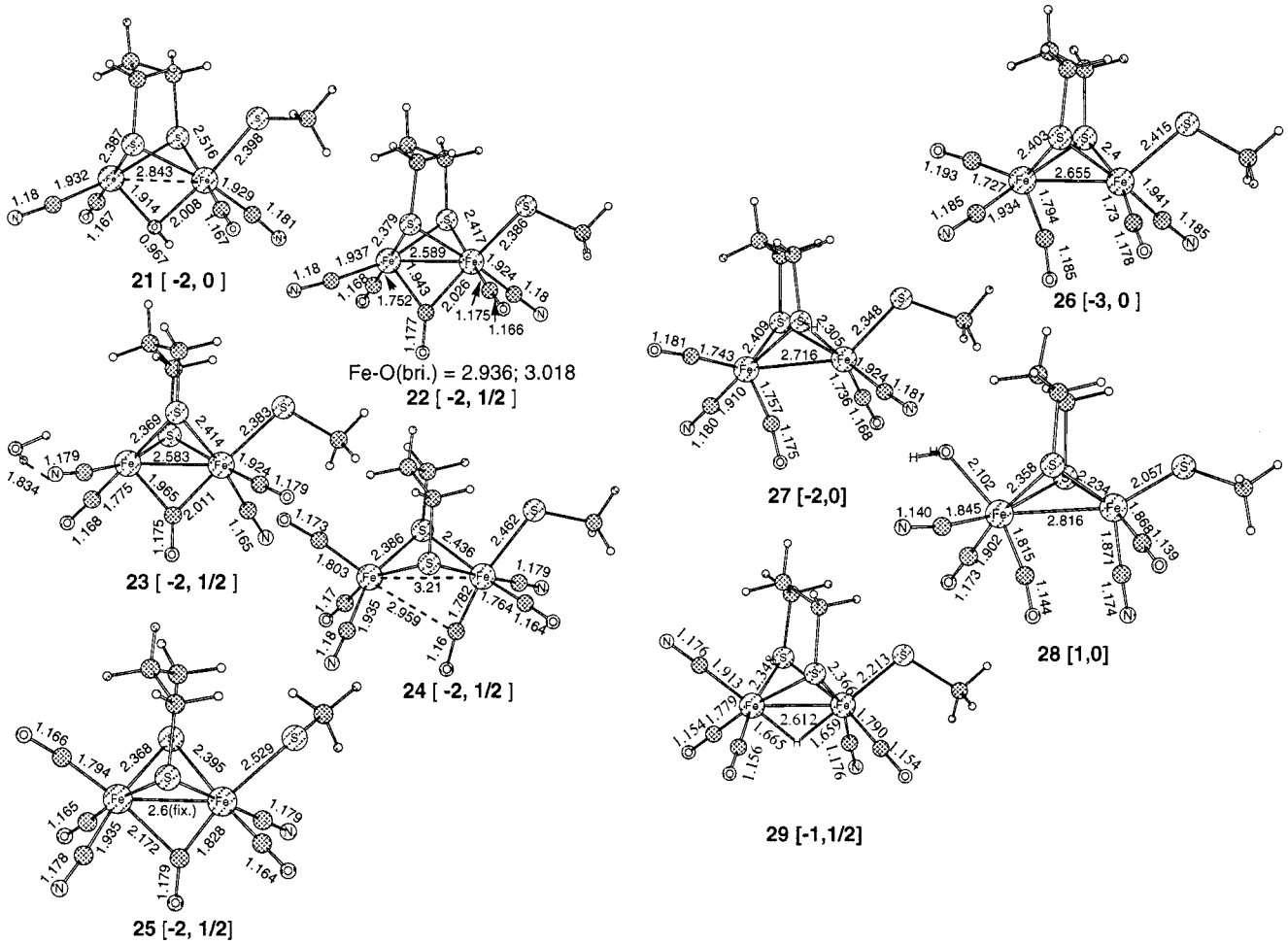

Figure 3. The DFT optimized geometries (Å, deg) of the diiron cluster candidates are shown with their charge (q) and spin (S), [q, S]. For our best models of the species determined by X-ray crystallography (**11** and **22**) we also give the Fe−O distances which may be compared to the experimental results in Figure 1.

precursor for the heterolytic cleavage of H_2 or for H_2 release after its formation from H^+ and e^-. In the (CO)Fe(II)-Fe(II) species **10**, the "bridging" CO moves away from Fe^d (with the new terminal CO) toward Fe^p and it shortens the C−O bond length to 1.159 Å, a value more characteristic of a terminal CO. The predicted frequency with major contribution from the "bridging" CO is 1974 cm^{-1}, higher than the corresponding predicted bridging bands at 1912 cm^{-1} of the Fe(II)-Fe(II) species **3**.

Partially Reduced States with $S = {}^1/_2$ EPR Signal. The Fe(I)-Fe(II)′ species **11** and the Fe(I)-Fe(II) species **22** can be considered as products of gradual reduction of the Fe(II)-Fe(II) species **3**. Although the predicted CN^- and CO bands of **11** presented in Table 3 appear to be a good match to experimental bands of the DvHase enzyme in air, this species cannot be assigned to the oxidized inactive enzyme due to the predicted EPR signal ($S = {}^1/_2$). These CN^- and terminal CO bands, 2108, 2104, 2000, and 1979 cm^{-1}, of **11** may be correlated with experimental bands at 2095, 2079, 1972, and 1965 (or 1940) cm^{-1} from a mixture of partially reduced DvHase [Fe]-hydrogenase[10] after complete replacement of H_2 by Ar, respectively. The very weak band at 2016 cm^{-1} may be due to some unreduced enzyme. The Fe(I)-Fe(II)′ species **11** binds H_2 to the empty site with an exothermicity of only −4 kcal/mol to form **13**. DFT calculations show that association of CO to the empty site of **11** results in dissociation of the $HSCH_3$ group, and that a complex with H_2O coordinated to the empty site decays to species **12**, which has a binding energy of 6.1 kcal/mol for the hydrogen-bonded interaction between the H_2O and CN^- ligand.

The predicted CN^- bands at 2093 and 2085 cm^{-1} and the terminal CO bands at 1950 and 1932 cm^{-1} of the Fe(I)-Fe(II) species **22** are lower than the FTIR bands of the oxidized enzyme.[10] These predicted bands match the observed CN^- and CO bands at 2079, 2041, 1941, and 1916 cm^{-1} of a mixture from the gradual H_2 reduction of the oxidized [Fe]-hydrogenase.[10] Experimentally, the 1940-cm^{-1} band observed in DvHase [Fe]-hydrogenase after complete replacement of H_2 by Ar was suggested to be characteristic of the EPR-detectable state.[10] The predicted CO bands of 1950 cm^{-1} of the Fe(I)-Fe(II) species **22** and 1979 cm^{-1} of the Fe(I)-Fe(II)′ species **11** are both close to the observed 1940 cm^{-1}. Therefore, both species with $S = {}^1/_2$ are candidates for the EPR-detectable state. Reasonable agreement in the geometry of **11** and **22** in Figure 3 and the crystal structure of DdHase[12] in Figure 1 also supports this assignment. Spin populations of **11** and **22** reveal that the unpaired electron is centered on Fe^d, the one with a empty coordination site. This is in agreement with the experimental conclusion that the unpaired spin is centered on the Fe distal to [4Fe-4S].[13] We also investigated a species with a bridging oxygen as has been presumed experimentally.[12] In species **21** with a bridging OH^-, the distances of Fe−O(bridging) are much smaller than those reported in the crystal structure (Figure 1), a result which suggests that oxygen as the bridging "X" is unlikely and CO as proposed by others[11,10] is a much better

Table 3. Comparison of Predicted CN and CO Frequencies (cm^{-1}) and Observed FTIR Bands in [Fe]-Hydrogenase

	predicted		observed[a]	
species	CN	CO	CN	CO
1 [0, 1/2]	2135	2089		
Fe(III)-Fe(II)	2127	2065		
		2056		
2 [0, 0]	2133	2085		
Fe(II)-Fe(II)′	2125	2052		
		2035		
3 [−1, 0]	2126	2030	2106[b]	2008
Fe(II)-Fe(II)	2105	2019	2087	1983
		1912		1848
4 [−1, 0]	2125	2009		
(H_2O)Fe(II)−Fe(II)	2102	1995		
		1945		
10 [−1, 0]	2131	2043		
(CO)Fe(II)-Fe(II)	2127	2010		
		1992		
		1974		
11 [−1, 1/2]	2108	2000	2095[c]	1972 (2016)
Fe(I)-Fe(II)′	2104	1979	2079	1965 (1940)
		1881		
17 [−2, 0]	2068	1912		
Fe(I)-Fe(I)′	2058	1882		
		1757		
18 [−2,0]	2087	1927	2079[d]	1916 (1965)
Fe(I)-Fe(I)′	2058	1886	2041	1894 (1941)
		1865		
21 [−2,0]	2087	1945		
Fe(II)-Fe(II)	2082	1936		
22 [−2, 1/2]	2093	1950	2079[d]	1941 (1965)
Fe(I)-Fe(II)	2085	1932	2041	1916 (1894)
		1835		
24 [−2, 1/2]	2101	1985	2096[e]	2016
(CO)Fe(I)-Fe(II)	2087	1956	2088	(1971)
		1931		(1964)
		1871		1811
25 [−2, 1/2]	2103	1969	2096[e]	2016
(CO)Fe(I)-Fe(II)	2096	1950	2088	(1971)
		1915		(1964)
		1828		1811
26 [−3, 0]	2051	1878		
Fe(I)-Fe(I)	2044	1834		
		1789		

[a] Reference 10. [b] Oxidized enzyme in Air. [c] Gradual reduction mixture under H_2/Ar conditions. [d] Gradual reduction mixture under H_2 conditions. [e] Gradual reduction mixture under H_2/CO conditions.

structural fit. As in the case of the Fe(I)-Fe(II)′ species **11**, coordination of H_2O to the empty site in the Fe(I)-Fe(II) species **22** is unstable and this initial geometry decays to the hydrogen-bonded complex **23** with a binding energy of 16.4 kcal/mol in the DFT optimization.[31] Initial complexes of H_2 coordinated to **22** always decay to separated species during optimization, showing that the Fe(I)-Fe(II) species **22** cannot bind H_2.

Note that in the experimental study the bridging CO band of the oxidized enzyme in air (1848 cm^{-1}) disappeared in mixtures formed by the gradual reducing conditions of H_2/Ar and H_2, while a bridging CO band appears under H_2/CO condition and is shifted 37 cm^{-1} to lower frequency compared with the bridging CO band of air-oxidized enzyme.[10] Disappearance of the bridging CO band under H_2/Ar and H_2 conditions may arise from either a loss of intensity or, more likely, conversion of the bridging CO to a terminal CO during the gradual reduction. Intensity of the calculated bridging CO band only shows a small intensity decrease from 545 km/mol in the Fe(II)-Fe(II) species **3** to 479 km/mol in Fe(II)-Fe(II)′ species **11** and 512 km/mol in the Fe(I)-Fe(II) species **22**, while the conversion from bridging to terminal CO indeed occurs in the fully reduced form as we will demonstrate (vide infra).

To gain insight into the observed bands at 1811 cm^{-1} under H_2/CO condition, we optimized the complex of CO with Fe(I)-Fe(II), **22**. Coordination of CO to the empty site of the Fe(I)-Fe(II) species **22** results in a stable complex (CO)Fe(I)-Fe(II), **24**. Although bridging CO does not exist in the fully optimized structure **24**, a strong CO band is predicted at 1871 cm^{-1}, which is mainly due to the additional CO with a bond length of 1.173 Å, and is not far from the observed band of 1811 cm^{-1}. However, since **24** has a very long Fe−Fe distance of 3.21 Å, we considered a restraint from the protein backbone. In the complex with CO coordinated to **22**, where the Fe−Fe separation is fixed at 2.6 Å, **25**, the bridging CO in the optimized structure has a bond length of 1.179 Å. A predicted bridging CO band at 1828 cm^{-1} in **25** is even a better match for the observed 1811-cm^{-1} band. This restrained structure, **25**, is only ~6 kcal/mol less stable than **24**. As in the oxidized species with additional CO, **10**, the bridging CO in **24** and **25** moves away from Fe^d toward Fe^p. Note that this motion is in agreement with that observed by Lemon and Peters[32] in the crystallography of the CO-inhibited enzyme and its photolysis product.

Completely Reduced EPR Silent States. The Fe(I)-Fe(I)′ species **17** and **18** and the Fe(I)-Fe(I) species **26** are plausible forms for the fully reduced diiron center. The Fe(I)-Fe(I)′ structure **17** can be easily converted to the Fe(I)-Fe(I)′ structure **18** without bridging CO: **18** is more stable than **17** by only −1.4 kcal/mol. Thus, structure **18** without bridging CO may be the stable form of the completely reduced enzyme. This is in agreement with the fact that no bridging CO band was observed experimentally in highly reduced mixtures of the *D. vulgaris* [Fe]-hydrogenase.[10] Association of H_2O to **17** does not form a stable (H_2O)Fe(I)-Fe(I)′ coordination complex; the H_2O migrates away from Fe and hydrogen bonds to CN^-, **19**. This hydrogen-bonded complex **19** is more stable than separated species by 18.0 kcal/mol.[31] The predicted CN^- bands at 2087 and 2058 cm^{-1} and predicted CO bands at 1927 and 1886 cm^{-1} of the Fe(I)-Fe(I)′ species **18** are close to the observed CN^- and CO bands of 2079, 2041, 1916, and 1894 cm^{-1} which appear in the *D. vulgaris* [Fe]-hydrogenase[10] after complete reduction by H_2. The predicted CN^- and CO frequencies of an alternative candidate, the Fe(I)-Fe(I) species **26**, are too low compared to the observed FTIR bands.

Reaction Mechanism at the Diiron Center. (a) Activation of the Oxidized Inactive State. Figure 3 shows the structure of the oxidized Fe(II)-Fe(II) species **3** which can bind H_2O to form the stable (H_2O)Fe(II)-Fe(II) species **4**, where H_2O occupies the previously empty coordinate site of **3**. Thus, the presence of strongly Fe-bound H_2O (23 kcal/mol) in the active site may be the origin of inactivity of the oxidized inactive [Fe]-hydrogenase. Gradual reduction of the (H_2O)Fe(II)-Fe(II) species **4** results in formation of complexes H_2O- - -Fe(I)-Fe(II)′, **12**, and H_2O- - -Fe(I)-Fe(II), **23**. In both species, **12** and **23**, the Fe-bound H_2O transfers to the spectator ligand CN^- (or in the enzyme it could return to some other part of the H-bonded network) and makes the active site available for dihydrogen binding. Thus, reduction from Fe(II)-Fe(II) to Fe(I)-Fe(II) releases the H_2O, which was blocking the active site. This step may be the "key" in the mechanism by which the oxidized inactive [Fe]-hydrogenase is activated upon reduction as observed experimentally.[27]

(31) This number is artificially large because species are unsolvated dianions in the calculation.

(32) Lemon, B. J.; Peters, J. W. *J. Am. Chem. Soc.* **2000**, *122*, 3793.

Scheme 1

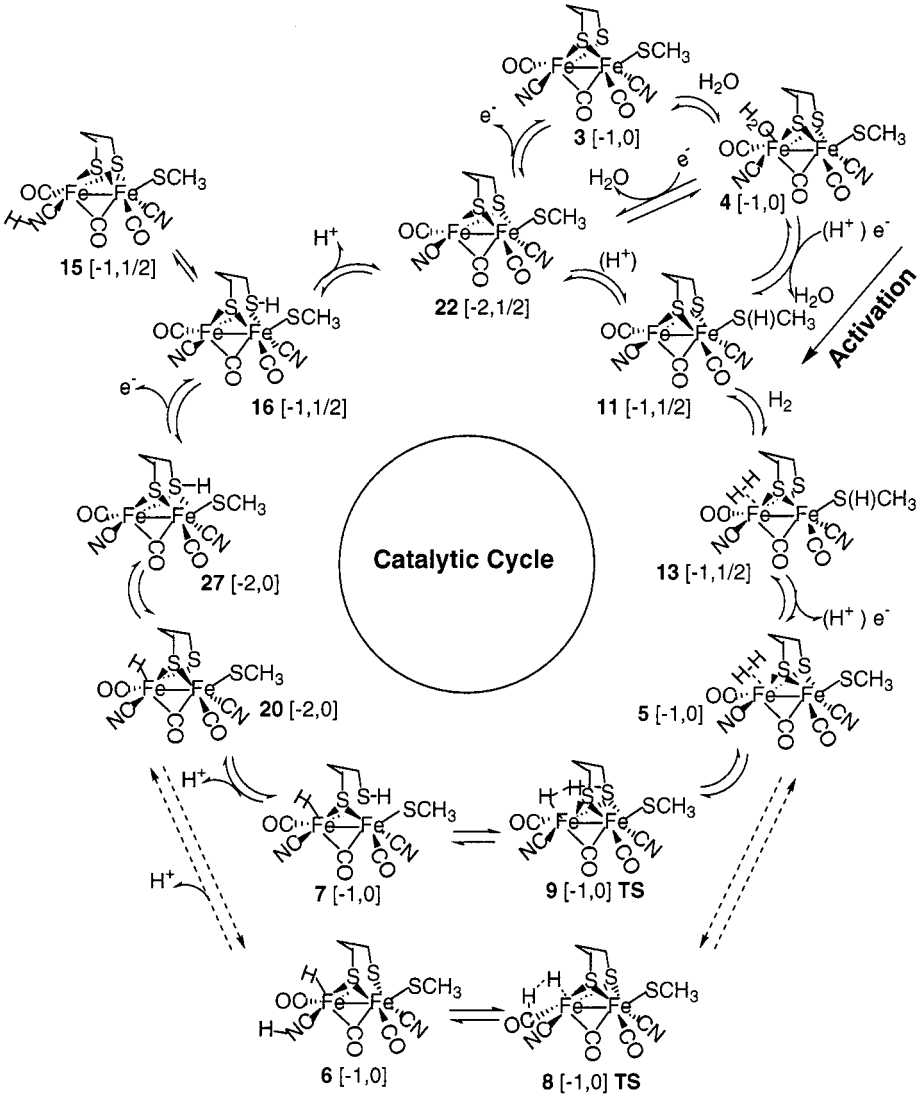

(b) Heterolytic Cleavage of H_2 and Proton Transfer. The Fe(I)-Fe(II)′ species **11** and the Fe(I)-Fe(II) species **22** with empty coordination sites at the diiron center may be active states for catalyzing the reversible reaction $H_2 \leftrightarrow 2H^+ + 2e^-$. The former can serve as a precursor for catalytic oxidation of H_2 while the latter may be a precursor for catalytic reduction of H^+. Scheme 1 displays a plausible catalytic reaction cycle at the diiron center, including activation of the oxidized inactive [Fe]-hydrogenase, binding and heterolytic cleavage of H_2, and proton and electron transfers at the diiron center ($H_2 \rightarrow 2H^+ + 2e^-$ is clockwise in Scheme 1).

Addition of H_2 to **11** results in formation of the (η^2-H_2)Fe-(II)-Fe(I)′ species **13** with an exothermicity of −6.1 kcal/mol. The EPR-active **13** is converted to an EPR-silent Fe(II)-Fe(II) species through an electron transfer (oxidation) and perhaps proton transfer to form **5**. Two possible paths for dissociation of H_2 on **5** were investigated, one involving Fe^d and S and the other involving Fe^d and CN. The calculated Mulliken charge densities (Table 4, hydrogens summed into heavy atoms) on relevant Fe^d, ligand CN^-, and S of the bridging PDT show that for the cleavage products **6** and **7** electron densities on Fe^d increase while electron densities on CN^- and S significantly decrease. These results support a view of heterolytic cleavage, $H_2 \rightarrow H^- + H^+$, where a hydride is left on Fe^d and a proton is transferred to CN^-, S, or some other basic protein site.

Table 4. Calculated Mulliken Charges on Fe, CN^-, and Bridging S

		Fe	CN^-	S
5	(η^2-H_2)Fe(II)-Fe(II)	−0.68	−0.24	0.22
6	HFe(II)(CNH)-Fe(II)	−0.77	0.15	
7	HFe(II)(μ-SH)-Fe(II)	−0.88		0.44

Heterolytic cleavage of H_2 was postulated to be involved in the enzymatic cycle of H_2.[17,18a,b] The cleavage product **6** is slightly more stable than **5** (0.3 kcal/mol), while **7** is 15.3 kcal/mol less stable than **5**. The barrier for conversion from **5** to **6** via the transition state **8** is about 37.8 kcal/mol, while **5** proceeds to **7** through transition state **9** with a relatively low barrier of 17.4 kcal/mol. Therefore, the proton transfer to the CN^- ligand is thermodynamically favorable but kinetically unfavorable over the proton transfer to bridging thiolates of the PDT.

Additional proton transfer from the cleavage products **6** and **7** leads to the Fe(II)-Fe(II) hydride species **20,** which isomerizes to **27**. This isomerization results in a "key" two-electron reduction at the metals that promotes subsequent electron transfer (oxidation) from **27** to **16**. Although we show a transfer to S in the isomerization (**20** → **27**), as for the initial heterolytic cleavage, CN or another base in the protein could be involved directly or at a later stage (**16** → **15**). Furthermore, an isomer of **15**/**16** with an Fe−H−Fe bridge, **29**, is even more stable

and similar species with a protonated Fe−Fe bond could be involved if the protein could accommodate such species.[18b−d] Final proton transfer from **15**/**16** to residues of the enzyme forms the Fe(I)-Fe(II) species, **22**, which is a ready state for reduction of H^+. The oxidized inactive form, (H_2O)Fe(II)-Fe(II) **4**, is formed through an electron transfer from **22** yielding **3**, followed by association of H_2O.

Conclusions

Spectroscopic properties and structural features of the diiron cluster model (L)(CO)(CN)Fe(μ-PDT)(μ-CO)Fe(CO)(CN)(L′) in various redox states were investigated by DFT calculations. By combining the observed FTIR spectra of [Fe]-hydrogenase and model systems similar to the diiron cluster in the enzyme with DFT computational results, possible redox states and their structures were determined. The oxidized inactive *D. vulgaris* [Fe]-hydrogenase as isolated in air is predicted to be an Fe(II)-Fe(II) species. The presence of H_2O strongly coordinated to the empty site of the Fe(II)-Fe(II) species is predicted to be the origin of inactivity of the oxidized inactive enzyme. Fe(I)-Fe(II) species and Fe(I)-Fe(I) species are responsible for the active EPR-detectable state and the fully reduced EPR-silent state, respectively. In the completely reduced Fe(I)-Fe(I) form, the structure without bridging CO is slightly more stable than species with bridging CO. The conversion of the bridging CO to a terminal CO may result in a completely reduced EPR-silent inactive form. An Fe(I)-Fe(II)′ species **11** can weakly bind H_2 and it may be a ready state for oxidation of H_2. The Fe(I)-Fe(II) species **22** cannot bind H_2 and it may be a precursor for reduction of H^+. Both can account for the active form of enzyme with the $S = {}^1/_2$ EPR signal.

Overall, there is excellent correlation (correlation coefficient 0.964, Figure 4) between the predicted frequencies determined in this work and previously measured FTIR bands for the various redox states of [Fe]-hydrogenase. DFT calculations show that protonation of CH_3S^- to form the CH_3SH ligand, as the model for the terminal Cys-S-[4Fe-4S], may simulate the electron-buffer role of the [4Fe-4S] cube during the redox process or other environmental changes as in H-bonding or solvation.

Reduction of the oxidized inactive form, (H_2O)Fe(II)-Fe(II), results in transfer of H_2O from the active site and formation of the active form containing an Fe(I)-Fe(II) pair. DFT calculations reveal that cleavage of H_2 in the (η^2-H_2)Fe(II)-Fe(II) species **5** is a heterolytic process, where the proton could be transferred to the bridging S of PDT. Proton transfer to the S is kinetically more favorable than proton transfer to CN^- ligand although CN or another base could be involved.

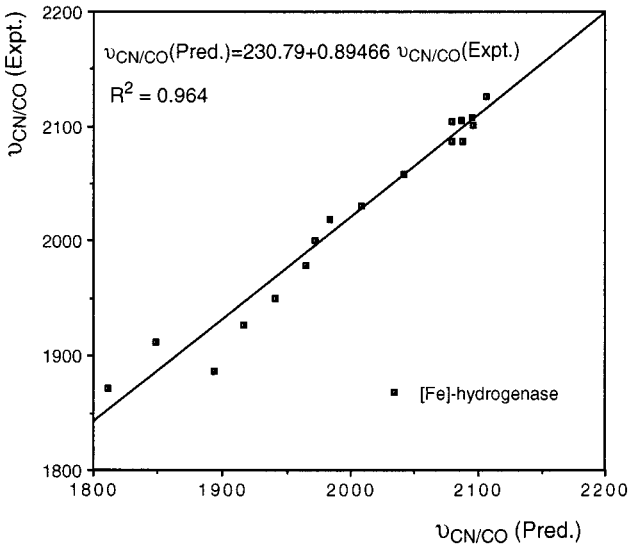

Figure 4. The predicted frequencies for the diiron cluster candidates are correlated with the observed bands in the enzyme.

Formation of H_2 from H^+ and e^- at the diiron center can proceed from **22** to **11** following the reverse of the oxidation mechanism ($2H^+ + 2e^- \rightarrow H_2$ is counterclockwise in Scheme 1). Note that the formation of H_2 from **7** to **5** has a very low barrier of 2.1 kcal/mol, and release of H_2 from **13** has an endothermicity of only ∼4 kcal/mol.

Acknowledgment. We gratefully acknowledge the National Science Foundation (Grant No. CHE-9800184) and The Welch Foundation (Grant No. A-648) for financial support of this work.

Note Added in Proof: Our prediction that in the fully reduced Fe(I)−Fe(I) form of the active site the bridging CO becomes essentially terminal has been confirmed by x-ray crystallography (Nicolet, Y.; De Lacey, A. L.; Vernède, X.; Fernandez, V. M.; Hatchikian, E. C.; Fontecilla-Camps, J. C. *J. Am. Chem. Soc.* **2001**, *123*, 1596). Recent work in our laboratory shows that using $(SCH_2)_2NH$ as a bridging ligand rather than $(SCH_2)_2CH_2$ provides a favorable low energy path for proton transfer (Fan, H.-J.; Hall, M. B. *J. Amer. Chem. Soc.* **2001**, in press).

JA000116V